Decreased cardiac L-type Ca^{2+} channel activity induces hypertrophy and heart failure in mice

Sanjeewa A. Goonasekera,[1] Karin Hammer,[2] Mannix Auger-Messier,[1] Ilona Bodi,[1] Xiongwen Chen,[3] Hongyu Zhang,[3] Steven Reiken,[4] John W. Elrod,[1] Robert N. Correll,[1] Allen J. York,[1] Michelle A. Sargent,[1] Franz Hofmann,[5] Sven Moosmang,[5] Andrew R. Marks,[4] Steven R. Houser,[3] Donald M. Bers,[2] and Jeffery D. Molkentin[1]

[1]Department of Pediatrics, University of Cincinnati, Cincinnati Children's Hospital Medical Center, Howard Hughes Medical Institute, Cincinnati, Ohio, USA. [2]Department of Pharmacology, UCD, Davis, California, USA. [3]Department of Physiology, Temple University School of Medicine, Philadelphia, Pennsylvania, USA. [4]Department of Physiology and Cellular Biophysics, College of Physicians and Surgeons of Columbia University, New York, New York, USA. [5]Munich Center for Integrated Protein Science, Munich, Germany, and Institut für Pharmakologie und Toxikologie, Technische Universität München, Munich, Germany.

Antagonists of L-type Ca^{2+} channels (LTCCs) have been used to treat human cardiovascular diseases for decades. However, these inhibitors can have untoward effects in patients with heart failure, and their overall therapeutic profile remains nebulous given differential effects in the vasculature when compared with those in cardiomyocytes. To investigate this issue, we examined mice heterozygous for the gene encoding the pore-forming subunit of LTCC (calcium channel, voltage-dependent, L type, α1C subunit [*Cacna1c* mice; referred to herein as $\alpha 1C^{-/+}$ mice]) and mice in which this gene was loxP targeted to achieve graded heart-specific gene deletion (termed herein *α1C-loxP* mice). Adult cardiomyocytes from the hearts of $\alpha 1C^{-/+}$ mice at 10 weeks of age showed a decrease in LTCC current and a modest decrease in cardiac function, which we initially hypothesized would be cardioprotective. However, $\alpha 1C^{-/+}$ mice subjected to pressure overload stimulation, isoproterenol infusion, and swimming showed greater cardiac hypertrophy, greater reductions in ventricular performance, and greater ventricular dilation than $\alpha 1C^{+/+}$ controls. The same detrimental effects were observed in *α1C-loxP* animals with a cardiomyocyte-specific deletion of one allele. More severe reductions in α1C protein levels with combinatorial deleted alleles produced spontaneous cardiac hypertrophy before 3 months of age, with early adulthood lethality. Mechanistically, our data suggest that a reduction in LTCC current leads to neuroendocrine stress, with sensitized and leaky sarcoplasmic reticulum Ca^{2+} release as a compensatory mechanism to preserve contractility. This state results in calcineurin/nuclear factor of activated T cells signaling that promotes hypertrophy and disease.

Introduction

Voltage-gated L-type Ca^{2+} channels (LTCCs) are the primary source of Ca^{2+} influx to initiate cardiac excitation-contraction coupling (ECC) (1, 2). The molecular composition of the LTCC in cardiomyocytes includes the pore-forming α1C subunit (*Cacna1c*; referred to herein as α1C), the β subunit, the $\alpha_2\delta$ subunit, and the more recently suggested γ subunit (3–6). The auxiliary subunits β, $\alpha_2\delta$, and γ are involved in trafficking the pore-forming α1C subunit to the sarcolemma and modulating the voltage dependence of channel gating (1). Genetic deletions of either the α1C or the β2 encoding genes results in embryonic lethality with heart dysfunction (7, 8).

Ca^{2+} influx via α1C triggers a much larger Ca^{2+} release from the sarcoplasmic reticulum (SR) via ryanodine receptors (RyRs) to promote myocyte contraction (9). In addition to regulating cardiomyocyte contraction, Ca^{2+} influx from LTCCs is also involved in intracellular signaling and gene regulatory events that underlie cardiac hypertrophy and disease (10–13). For example, multiple studies have suggested that enhanced Ca^{2+} influx via the LTCC is responsible for cardiac hypertrophy and pathological remodeling of the ventricles (14–16). Consistent with these observations, LTCC blockers effectively inhibit cardiac remodeling and disease after pressure overload stimulation in animal models (17–19). However, α1C is also widely expressed in the vasculature, and the net beneficial cardiovascular effects of LTCC inhibitors in animal models could result from changes in vascular compliance and/or function to secondarily benefit the heart (15). In human clinical trials, LTCC blockers appear to either have no effect or to negatively impact the survival and cardiovascular event profile in patients with heart failure with systolic dysfunction (20). Thus, it remains unclear how LTCC inhibitors might be of clinical importance in heart failure as well as the cell type that mediates beneficial compared with detrimental effects.

Many studies have documented an association between increased Ca^{2+} influx during cardiac stress states and the induction of hypertrophy. Thus, we tested the hypothesis that a genetic reduction in LTCC current would reduce Ca^{2+} influx and thereby protect the heart during disease-causing stress stimulation, consistent with animal models treated with LTCC blockers that show less hypertrophy. However, we observed the opposite effect and show that reductions in cardiomyocyte LTCCs cause a compensatory increase in neuroendocrine stimulation and RyR2 Ca^{2+} leak toward increasing the gain in ECC, resulting in pathologic cardiac hypertrophy and failure through calcineurin/nuclear factor of activated T cells (calcineurin/NFAT) signaling.

Conflict of interest: The authors have declared that no conflict of interest exists.
Citation for this article: *J Clin Invest.* 2012;122(1):280–290. doi:10.1172/JCI58227.

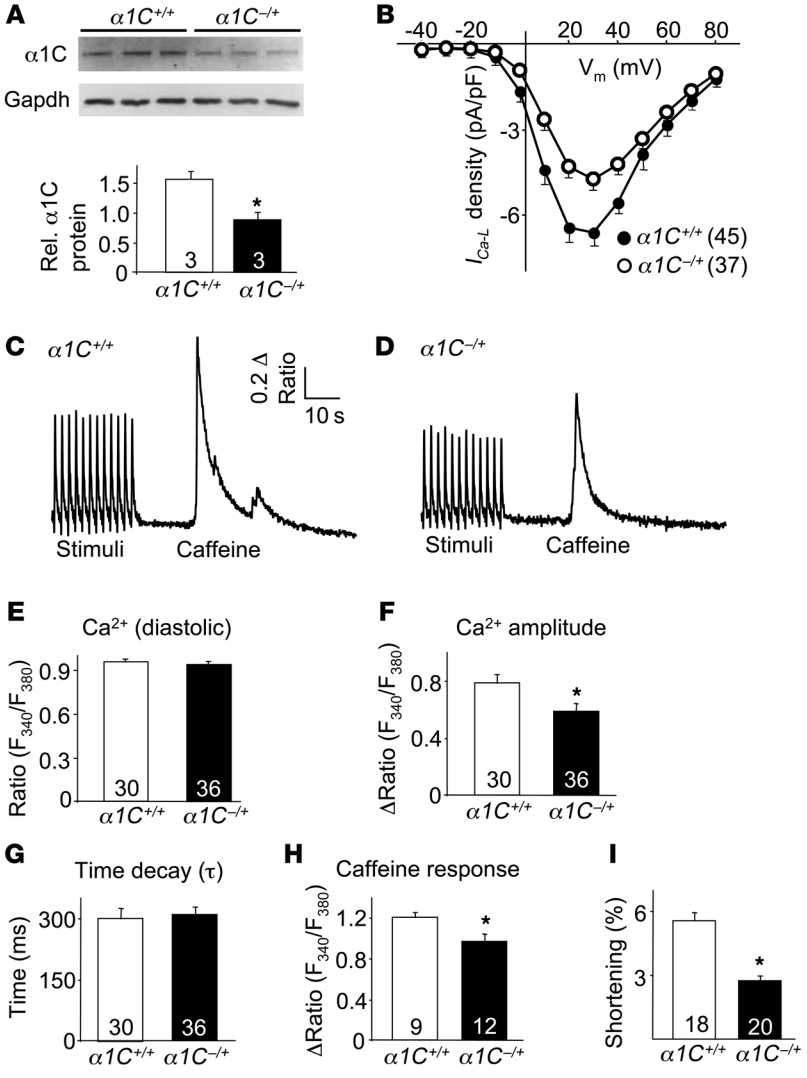

Figure 1
Decreased $I_{Ca\text{-}L}$ density in $\alpha 1C^{-/+}$ myocytes results in a modest deficit in cardiac ECC. (**A**) Western blotting and quantitation α1C protein expression of hearts of $\alpha 1C^{+/+}$ and $\alpha 1C^{-/+}$ mice at 10 weeks of age. Gapdh is shown as a control. Rel, relative. (**B**) Voltage dependence of average maximal $I_{Ca\text{-}L}$ density (V_m) measured in whole-cell patch clamp experiments in myocytes isolated from $\alpha 1C^{+/+}$ and $\alpha 1C^{-/+}$ mice. (**C** and **D**) Representative traces of F_{340}/F_{380} fluorescence ratio recordings in $\alpha 1C^{+/+}$ and $\alpha 1C^{-/+}$ myocytes. (**E**) Resting Ca^{2+}, (**F**) average maximal amplitude of electrically evoked Ca^{2+} transients, (**G**) time constant of Ca^{2+} decay (τ), and (**H**) average maximal Ca^{2+} response to a 10 mM caffeine bolus in myocytes from the indicated genotypes. (**I**) Percentage of shortening of adult myocytes from the hearts of the indicated genotypes of mice. *$P < 0.05$ compared with $\alpha 1C^{+/+}$. At least 3 animals were used, and the total number of cells analyzed is shown on bars in the graphs and in parentheses otherwise.

Results

Baseline characterization of mice heterozygous for α1C. Given the protective effects associated with LTCC inhibitors in animal models of heart failure and hypertrophy, we hypothesized that $\alpha 1C^{-/+}$ mice would be protected from heart failure secondary to cardiac injury. Cardiac protein levels of α1C were reduced by approximately 40% in $\alpha 1C^{-/+}$ mice compared with those in control mice at 10 weeks of age (Figure 1A), which correlated with roughly 25% less whole-cell L-type Ca^{2+} current ($I_{Ca\text{-}L}$) measured in freshly isolated adult ventricular myocytes (Figure 1B). No changes in cell capacitance were observed (data not shown). Ca^{2+} photometry experiments showed that the maximal amplitude of electrically evoked (Figure 1, C, D, and F) and caffeine-evoked (Figure 1, C, D, and H) Ca^{2+} transients was significantly reduced in $\alpha 1C^{-/+}$ adult cardiomyocytes compared with that in WT cardiomyocytes, with no noticeable changes in diastolic Ca^{2+} or the decay time constant for Ca^{2+} reuptake and extrusion (Figure 1, E and G). Associated with these reductions in Ca^{2+} handling, myocyte shortening (Figure 1I) and ventricular fractional shortening (FS) were also reduced in $\alpha 1C^{-/+}$ mice compared with those in WT mice (Figure 2A), as was cardiac $+dP/dt$, measured ex vivo with a Millar pressure transducing catheter (Figure 2B). This mild reduction in cardiac performance in $\alpha 1C^{-/+}$ mice was also associated with increased left ventricular chamber size in systole at 10 and 32 weeks of age (Figure 2C), which eventually resulted in a small but significant induction of cardiac hypertrophy by 32 weeks of age, as assessed by measurement of heart weight normalized to body weight (HW/BW; Figure 2D).

$\alpha 1C^{-/+}$ mice develop greater cardiac disease after pathologic or physiologic stress. To further examine the cardiac effects associated with a reduction in LTCC current, $\alpha 1C^{-/+}$ mice at 10 weeks of age, which is prior to an increase in heart weight, were subjected to pathologic and physiologic hypertrophic stimulation. Again, since increased Ca^{2+} influx has been associated with cardiac hypertrophy and pathological remodeling, we initially hypothesized that reduced whole-cell LTCC current would be cardioprotective in mice subjected to pressure overload by transverse aortic constriction (TAC). However, $\alpha 1C^{-/+}$ mice subjected to TAC for 2 weeks exhibited enhanced cardiac remodeling, demonstrated by increased HW/BW (Figure 3A), reduced cardiac ventricular performance (Figure 3B), and ventricular chamber dilation, compared with that in $\alpha 1C^{+/+}$ mice (Figure 3C). To extend these observations, we used a model of catecholamine overload-induced disease with 2 weeks of isoproterenol (Iso) infusion. Consistent with

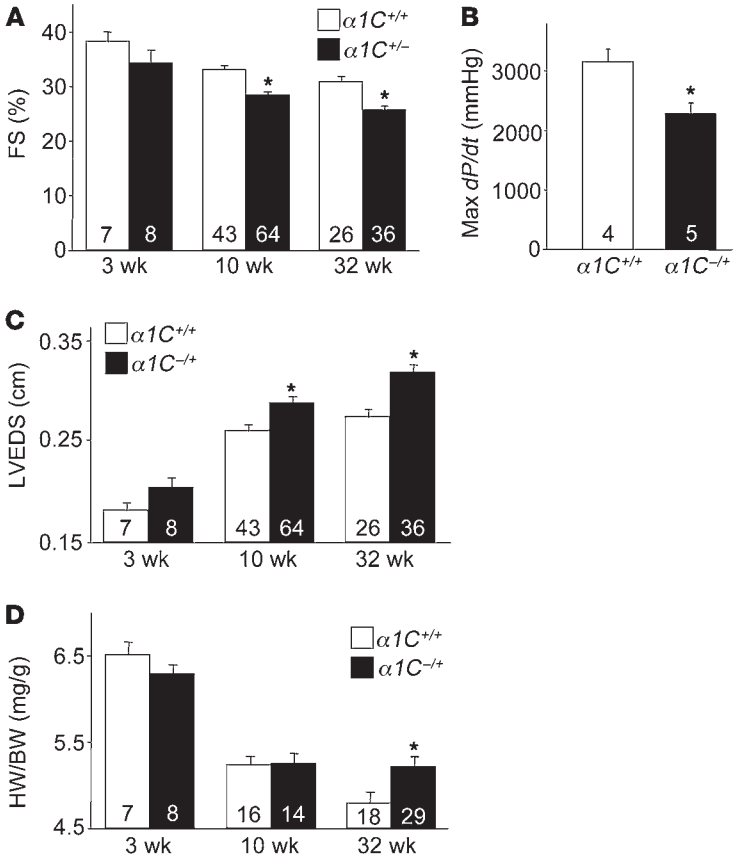

Figure 2
Decreased $I_{Ca\text{-}L}$ density leads to age-dependent remodeling of the $\alpha 1C^{-/+}$ mouse myocardium. (**A**) Echocardiographic assessment of the FS percentage in hearts of $\alpha 1C^{+/+}$ and $\alpha 1C^{-/+}$ mice at the indicated ages. (**B**) Assessment of cardiac contractility in $\alpha 1C^{+/+}$ and $\alpha 1C^{-/+}$ mice at 10 weeks of age with a Millar catheter. (**C**) Echocardiographic assessment of left ventricular end dimension at systole (LVEDS) in $\alpha 1C^{+/+}$ and $\alpha 1C^{-/+}$ mice at the indicated ages. (**D**) Heart weight to body weight (HW/BW) ratio as a function of time in $\alpha 1C^{+/+}$ and $\alpha 1C^{-/+}$ mice. *$P < 0.05$ compared with $\alpha 1C^{+/+}$. The total number of animals used in each genotype is shown on bars in the graphs.

those in the TAC experiments, $\alpha 1C^{-/+}$ mice showed a minor but significant reduction in ventricular performance and increase in cardiac hypertrophy compared with that of $\alpha 1C^{+/+}$ littermates treated with Iso (Figure 3, D and E). Finally, and unexpectedly, $\alpha 1C^{-/+}$ mice also showed a significant reduction in ventricular performance and increased cardiac hypertrophy after exercise stimulation for 21 days by forced swimming (Figure 3, F and G). Collectively, these results indicate that decreased $I_{Ca\text{-}L}$ does not protect against cardiac hypertrophy after either pathologic or physiologic stimulation, but, to the contrary, it exacerbates disease.

To exclude the known effects of LTCC antagonists on the vasculature, we crossed α1C-loxP–targeted (floxed [fl]) heterozygous mice with transgenic mice expressing Cre recombinase under control of the α-myosin heavy chain (α-MHC) promoter (only 1 allele would be specifically deleted in cardiomyocytes). Echocardiographic analysis of $\alpha 1C^{+/fl\text{-}Cre}$ mice after 2 weeks of TAC showed a significant decrease in cardiac function and enhanced propensity for myocardial remodeling compared with that of controls ($\alpha 1C^{+/fl}$) (Supplemental Figure 1; supplemental material available online with this article; doi:10.1172/JCI58227DS1). Heart-specific $\alpha 1C^{+/fl\text{-}Cre}$ mice also showed greater decompensation and hypertrophy after swimming exercise for 21 days compared with that of controls, an effect that was not altered with an LTCC blocker, diltiazem (Supplemental Figure 1). Finally, we also crossed α1C-loxP heterozygous mice with α-MHC-MerCreMer transgenic mice to permit tamoxifen-inducible deletion of 1 α1C allele in the adult heart. Ten-week-old $\alpha 1C^{+/fl\text{-}MerCreMer}$ mice were given tamoxifen (25 mg/kg/d) for 5 days and then subjected to TAC 4 weeks later for 2 weeks. Importantly, these mice also showed a significant reduction in ventricular performance and ventricular dilation and an increase in hypertrophy compared with those in controls, again suggesting that myocyte-specific reduction in LTCC activity worsens cardiac disease after pathologic stimulation (Supplemental Figure 1).

Cardiac-specific and more complete deletion of α1C produces severe hypertrophy and remodeling. We were also interested in achieving an even greater reduction in LTCC current to better investigate the mechanism of disease predisposition observed in α1C heterozygous mice. We analyzed double α1C-loxP–targeted mice (2 floxed alleles) with the α-MHC-Cre transgene as well as single allele α1C-loxP mice (with Cre) over an α1C-null allele to achieve an even more complete knockdown of LTCC activity in the heart, which was verified by Western blotting (Figure 4A) and careful assessment of Ca^{2+} current from isolated myocytes of each of the genotypes (Supplemental Figure 2). Indeed, $\alpha 1C^{-/fl\text{-}Cre}$ mice had the greatest reduction in Ca^{2+} current, followed by $\alpha 1C^{fl/fl\text{-}Cre}$ mice, and then $\alpha 1C^{-/fl}$ mice (Supplemental Figure 2). We were unable to examine standard, fully deleted $\alpha 1C^{-/-}$ mice, because they are embryonically lethal (7). Use of the α-MHC-Cre transgene bypassed embryonic lethality in $\alpha 1C^{fl/fl}$ and $\alpha 1C^{-/fl}$ mice, due to its predominant postnatal expression characteristics.

Consistent with the degree of α1C protein and current reduction, $\alpha 1C^{fl/fl\text{-}Cre}$ mice and $\alpha 1C^{-/fl\text{-}Cre}$ mice showed partial adult lethality as they aged to 80 days (Figure 4B). Both $\alpha 1C^{fl/fl\text{-}Cre}$ and $\alpha 1C^{-/fl\text{-}Cre}$ mice showed a significant reduction in cardiac ventricular performance at 10 weeks of age compared with that of control mice (Figure 4C). The reduction in performance was significantly greater in $\alpha 1C^{-/fl\text{-}Cre}$ mice, which had the greatest reduction in α1C protein and current. Consistent with these results, $\alpha 1C^{fl/fl\text{-}Cre}$ and $\alpha 1C^{-/fl\text{-}Cre}$ mice each showed dramatic increases in left ventricular chamber dimensions and cardiac hypertrophy, which, again, were even more pronounced in the $\alpha 1C^{-/fl\text{-}Cre}$ genotype (Figure 4, D, E, and G). This dramatic increase in cardiac hypertrophy in $\alpha 1C^{-/fl\text{-}Cre}$ mice was also associated with heart failure, as assessed by increases in lung weight normalized to body weight (Figure 4F). These results suggest that reductions in Ca^{2+} influx induce cardiac hypertrophy and heart failure in young adult mice.

Calcineurin signaling in α1C-deleted mice. We originally hypothesized that a genetic reduction in α1C current would reduce the total amount of Ca^{2+} available to activate calcineurin/NFAT signaling, a pro-hypertrophic regulatory pathway in the heart, especially given previous work suggesting that enhanced LTCC activity mediates cardiac hypertrophy through Ca^{2+}-dependent signaling pathways (21). Thus, we first crossed NFAT-luciferase transgenic reporter mice with $\alpha 1C^{-/fl\text{-}Cre}$ mice, expecting to observe less activity.

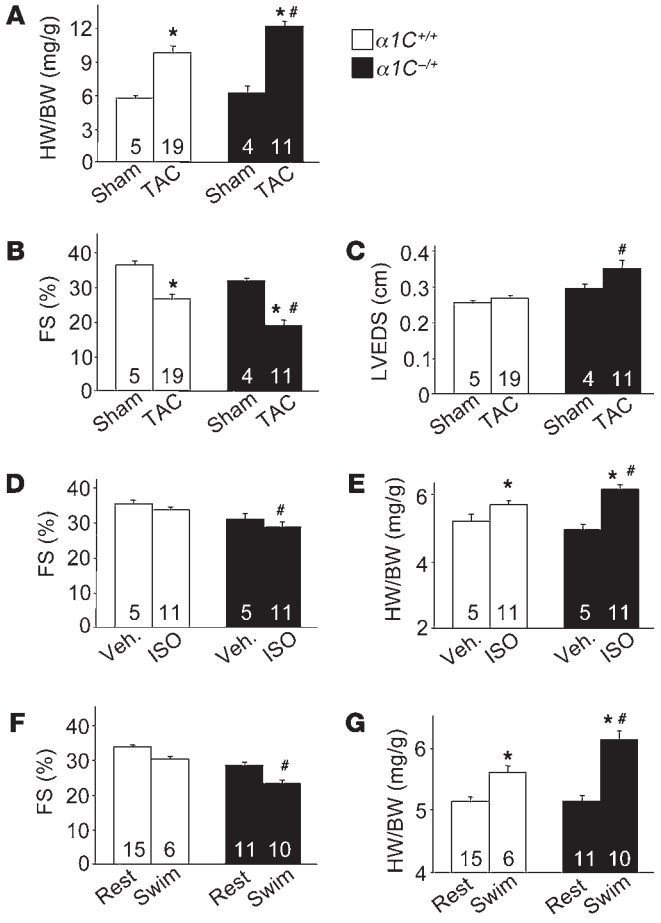

Figure 3
$\alpha 1C^{-/+}$ mice show greater cardiac decompensation in response to pathological or physiological stimuli. (**A**) HW/BW measured in 10-week-old $\alpha 1C^{+/+}$ and $\alpha 1C^{-/+}$ mice subjected to 2 weeks of cardiac pressure overload by TAC. (**B** and **C**) Echocardiographic measurements of FS and left ventricular end dimension at systole in $\alpha 1C^{+/+}$ and $\alpha 1C^{-/+}$ mice after 2 weeks of pressure overload. (**D**) Echocardiographic measurement of FS in $\alpha 1C^{+/+}$ and $\alpha 1C^{-/+}$ mice after 2 weeks of Iso or vehicle (Veh.) infusion, (**E**) followed by measurement of HW/BW. (**F**) Echocardiographic measurement of FS in $\alpha 1C^{+/+}$ and $\alpha 1C^{-/+}$ mice after 21 days of forced swimming exercise or rest, (**G**) followed by measurement of HW/BW. $^{*}P < 0.05$ compared with sham-operated, vehicle-treated, or resting $\alpha 1C^{+/+}$ mice; $^{\#}P < 0.05$ compared with $\alpha 1C^{+/+}$ mice subjected to TAC, Iso infusion, or swimming. The number of mice used in each experiment is shown on bars in the graphs.

However, consistent with the unexpected and profound induction of hypertrophy seen in $\alpha 1C^{-/fl\text{-}Cre}$ mice, we observed a large induction in cardiac NFAT activity and calcineurin phosphatase activity compared with that in control hearts (Figure 5, A and B). This suggested that a reduction in Ca^{2+} influx from the LTCC might lead to a secondary increase in Ca^{2+} that is important for activating calcineurin/NFAT signaling. Indeed, $\alpha 1C^{-/fl\text{-}Cre}$ mice treated for 3 weeks with cyclosporine A (CsA), a calcineurin inhibitor, showed partial but significant regression in ventricular dilation and hypertrophy and significantly (albeit minor) better cardiac function compared with that of untreated controls (Figure 5, C–E). These results suggest that reduced LTCC current leads to calcineurin/NFAT activation and cardiac hypertrophy with pathology.

SR Ca^{2+} cycling in α1C-deleted mice. Considering the results of our study to this point, we revised our hypothesis to indicate that there must be an increase in SR Ca^{2+} leak or greater resting Ca^{2+} levels in the cleft microenvironment to compensate for less trigger Ca^{2+}. This hypothetical increase in Ca^{2+} could then serve as a potent stimulus for reactive signaling pathways, such as calcineurin (22, 23). To assess this revised hypothesis, we measured Ca^{2+} handling in adult cardiomyocytes from $\alpha 1C^{-/fl\text{-}Cre}$ mice. As expected, the maximal amplitude of electrically evoked Ca^{2+} transients was significantly reduced in myocytes from $\alpha 1C^{-/fl\text{-}Cre}$ hearts and almost significantly reduced again in myocytes from standard heterozygous hearts ($\alpha 1C^{-/fl}$; compare with a larger sampling in Figure 1F) compared with that in controls (Figure 6A). The time constant of decay was significantly longer in myocytes from $\alpha 1C^{-/fl\text{-}Cre}$ hearts compared with that in control myocytes (Figure 6B). These changes were accompanied by a concomitant reduction in the SR Ca^{2+} load and peak release in both deficient genotypes (Figure 6C). However, the frequency of SR Ca^{2+} sparks measured in $\alpha 1C^{-/fl\text{-}Cre}$ myocytes was significantly higher than that in control myocytes (Figure 6D), despite a lower SR Ca^{2+} content. Consistent with this, independent measurements of tetracaine-sensitive diastolic SR Ca^{2+} leak (normalized for SR Ca^{2+} content) were also higher in $\alpha 1C^{-/fl\text{-}Cre}$ myocytes (Figure 6E). These data suggest that the SR Ca^{2+} release channel is sensitized, perhaps in compensation for the reduced Ca^{2+} entry via LTCC current. Indeed, in voltage-clamped myocytes in which SR Ca^{2+} load was matched among the groups (via longer loading pulses in $\alpha 1C^{-/fl\text{-}Cre}$ myocytes; Figure 6F) the Ca^{2+} transient peaks were not different among groups, despite the reduced Ca^{2+} trigger current in $\alpha 1C^{-/fl\text{-}Cre}$ myocytes (Figure 6G). More importantly, when normalized for Ca^{2+} current amplitude, there was increased gain of ECC in $\alpha 1C^{-/fl\text{-}Cre}$ hearts compared with that in control hearts (Figure 6H). This again suggests that the SR Ca^{2+} release channel is more sensitive to Ca^{2+} in the $\alpha 1C^{-/fl\text{-}Cre}$ myocytes.

RyR2 shows a pathologic profile that is corrected with beta blockers or CaMK inhibition. The increase in ECC gain and increased SR Ca^{2+} leak can be regulated by β-adrenergic receptor signaling through PKA and Ca^{2+}/calmodulin-dependent kinase II (CaMKII) (24–26). Such a profile is associated with hyperphosphorylation of RyR2 at serine 2808 and 2814, with less calstabin2 (FKBP12.6) binding to the channel. Indeed, hearts from $\alpha 1C^{-/fl\text{-}Cre}$ mice showed significantly greater phosphorylation of RyR2, with less calstabin2 binding, and profound oxidative nitrosylation (with 2,4-dinitrophenyl [DNP]) compared with that of α1C heterozygous controls (Figure 7, A–D). Given these results, we further reasoned that β-receptor blockade might limit the compensatory neurohumoral response that attempts to increase the gain in ECC, in part by phosphorylating RyR2, secondarily reducing this detrimental pool of Ca^{2+} that induces hypertrophy and disease. Hence, we treated $\alpha 1C^{+/+}$ and $\alpha 1C^{-/+}$ mice with the β_1-adrenergic receptor selective antagonist metoprolol and then subjected the mice to pressure overload. Metoprolol-treated $\alpha 1C^{-/+}$ mice maintained better cardiac ventricular performance and showed less ventricular dilation and less cardiac hypertrophy compared with vehicle-treated $\alpha 1C^{-/+}$ mice (Figure 7, E–G). Activation of CaMKII is also a consequence of β-receptor and neurohumoral activation that can cause increased RyR2 Ca^{2+} leak. Indeed, the CaMKII inhibitory drug

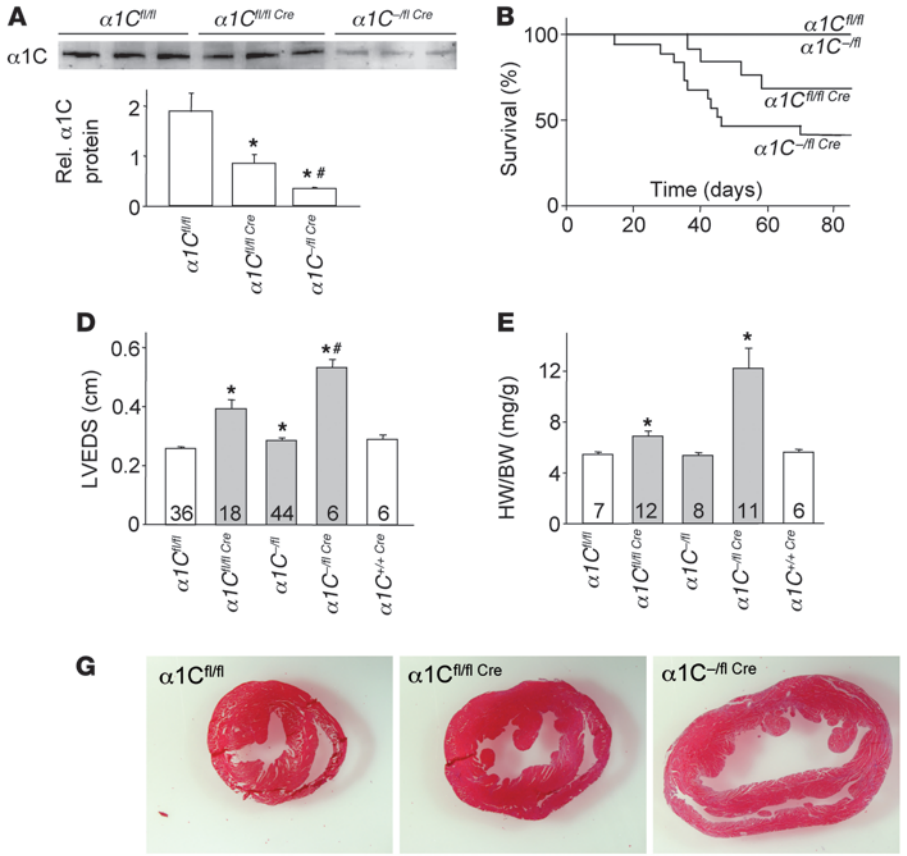

Figure 4

Dose-dependent decrease in α1C expression results in progressive cardiac dysfunction, myocardium remodeling, and death in mice. (**A**) Western blot and quantitation of α1C expression in α1C-homozygous-loxP–targeted mice (fl/fl mice) or mice with 1 loxP allele over a null allele (–/fl mice), both containing the α-MHC-Cre transgene. (**B**) Kaplan-Meier plots show survival rates in the indicated genotypes with aging. (**C** and **D**) Echocardiographic assessment of FS and left ventricular end dimension at systole in the indicated genotypes of mice at 2 months of age. (**E** and **F**) Gravimetric analysis of changes in HW/BW and lung weight to body weight ratio (LW/BW) in the indicated genotypes of mice at 2 months of age. (**G**) Representative transverse histological sections of mouse hearts of the indicated genotypes stained with H&E. Original magnification, ×10. *$P < 0.05$ compared with $\alpha 1C^{fl/fl}$; #$P < 0.05$ compared with $\alpha 1C^{fl/fl\ Cre}$. The number of mice used is shown on the bars in the graphs.

KN93 restored the detriment to the Ca^{2+} transient and SR Ca^{2+} content and prevented SR Ca^{2+} leak in myocytes from $\alpha 1C^{-/fl\text{-}Cre}$ hearts (Figure 7, H and I, and data not shown). These results again suggest that the neurohumoral response is engaged in $\alpha 1C^{-/fl\text{-}Cre}$ hearts in an attempt to compensate for less trigger Ca^{2+} but, in so doing, causes Ca^{2+} leak from RyR2 that induces pathological signaling and hypertrophy/heart failure.

We also crossed $\alpha 1C^{-/fl\text{-}Cre}$ mice with transgenic mice expressing the α1G subunit of the T-type Ca^{2+} channel (TTCC) to assess rescue in hypertrophic disease by enhancing trigger Ca^{2+} independent of the LTCC (27). Remarkably, α1G overexpression essentially rescued the secondary hypertrophy in $\alpha 1C^{-/fl\text{-}Cre}$ mice by providing more Ca^{2+} for acute systolic release (Supplemental Figure 3). α1G overexpression also mildly reduced ventricular remodeling in hearts from $\alpha 1C^{-/fl\text{-}Cre}$ mice, which was associated with a restoration in the Ca^{2+} transient and peak SR Ca^{2+} load (Supplemental Figure 3). Collectively, these results further suggest that a reduction in trigger Ca^{2+} is responsible for a compensatory increase in diastolic Ca^{2+} to increase ECC gain. Increased diastolic Ca^{2+} is a potent means of activating calcineurin.

Discussion

Increased Ca^{2+} influx via LTCCs has been implicated in the development of hypertrophy and pathological remodeling of the heart with select stress stimuli (15, 28). For example, studies in animal models of heart disease have shown that antagonizing LTCC activity with pharmacologic inhibitors can prevent or reverse pathological cardiac remodeling and hypertrophy (17–19). We previously showed that upregulation of LTCC activity in the hearts of transgenic mice due to overexpression of the β2a subunit induced cardiomyopathy (29). Total LTCC currents were increased by nearly 50% in adult myocytes from these hearts, which enhanced cardiac contractility and eventually caused necrotic death of myocytes, leading to dilated failure, with slightly heavier hearts. However, one perplexing observation from these mice was the relative lack of bona fide hypertrophy associated with enhanced Ca^{2+} influx, especially in mice that were less than 3 months old, as we initially hypothesized that such a dramatic increase in Ca^{2+} would induce calcineurin activation (29). Similarly, α1C-overexpressing transgenic mice did not show cardiac hypertrophy until 8 months of age, and then it was mild and possibly secondary to neurohumoral

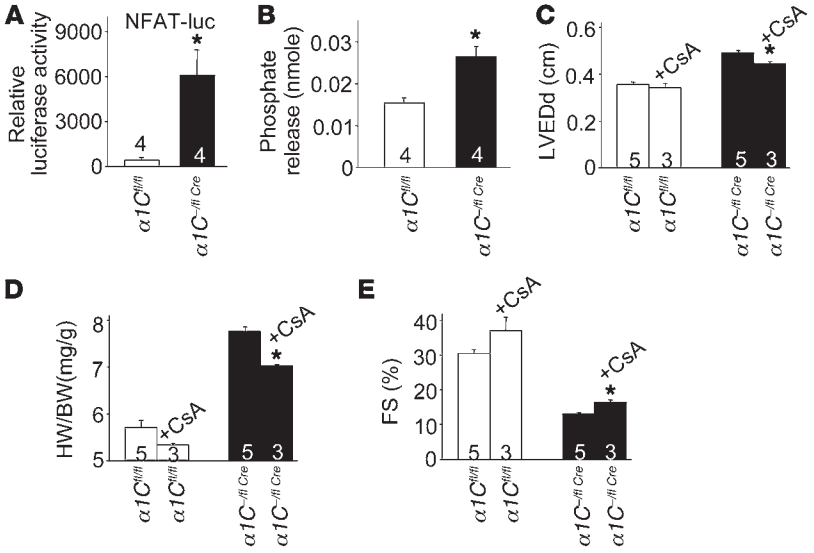

Figure 5
Decreased expression of α1C leads to calcineurin activation and calcineurin-dependent hypertrophy. (**A**) NFAT-luciferase activity assessed in cardiac lysates obtained from $\alpha 1C^{fl/fl}$ and $\alpha 1C^{-/fl\text{-}Cre}$ mouse hearts that also contain the NFAT-lucifease reporter transgene. *$P < 0.05$ compared with $\alpha 1C^{fl/fl}$. (**B**) Calcineurin phosphatase activity from $\alpha 1C^{fl/fl}$ and $\alpha 1C^{-/fl\text{-}Cre}$ mouse hearts. *$P < 0.05$ compared with $\alpha 1C^{fl/fl}$. (**C**) Assessment of ventricular dilation by echocardiography, (**D**) HW/BW, (**E**) and percentage of FS in $\alpha 1C^{fl/fl}$ and $\alpha 1C^{-/fl\text{-}Cre}$ mice treated with vehicle or CsA for 3 weeks, beginning at 4 weeks of age. LVEDd, left ventricular end diastolic dimension. *$P < 0.05$ compared with $\alpha 1C^{fl/fl}$. The number of mice analyzed is shown on the bars in the graphs.

effects (30, 31). Thus, increasing the peak or acute release of Ca^{2+} appears to be a weak inducer of hypertrophic disease and pathologic signaling, though it can lead to mitochondrial Ca^{2+} overload and cellular necrosis, leading to dilated heart failure, with slight increases in heart weight that are likely dilatory in nature (sarcomeres added in series) and secondary to neurohumoral status.

In contrast to the above interpretation, downregulation of the β2 subunit using a gene transfer strategy in aortic banded rats showed prevention of the hypertrophic response (32). However, this knockdown approach of β2 did not reduce systolic function in these animals, and α1C protein was not reduced compared with that in sham viral-injected hearts. Hence, it remains uncertain how these data relate to our observations in $\alpha 1C^{-/+}$ and $\alpha 1C^{fl/fl\text{-}Cre}$ mice that did show reduced current, α1C protein, and cardiac function. Indeed, Rosati et al. recently showed that heart-specific deletion of α1C resulted in reduced cardiac function and early postnatal lethality, although heterozygous deleted mice showed no baseline phenotype in their analysis (33). These disparities notwithstanding, perhaps the most important observations are from clinical trials with Ca^{2+} channel antagonists, which failed to show protective effects in patients with heart failure with systolic dysfunction and, in some cases, showed signs of worsening disease and increased mortality (34, 35). Thus, reducing Ca^{2+} influx through LTCCs in cardiomyocytes may not be a desirable therapeutic strategy for systolic heart failure, consistent with our observations of worsening disease due to graded deletion of α1C in our multiple genetic strategies.

We did not anticipate that a genetic-based reduction in LTCC current would induce spontaneous cardiac hypertrophy or dramatically enhance hypertrophy after pressure overload stimulation. Our new working hypothesis is that, in the absence of sufficient LTCC current, SR Ca^{2+} release is sensitized in an attempt to maintain cardiac contractility, leading to hypertrophic remodeling through calcineurin/NFAT activation. The reduction in cardiac function likely causes a compensatory neuroendocrine response through β-adrenergic receptors that in turn mediates PKA and CaMKII activation to phosphorylate nodal Ca^{2+} handling and contractile proteins in an attempt to augment contractility (36, 37). In this manner, phosphorylation of the LTCCs and RyR2s would attempt to compensate for the reduced Ca^{2+}-induced Ca^{2+} release relationship by allowing the RyR2 to leak and open with substantially less trigger Ca^{2+}. This would tend to elevate Ca^{2+} in the cleft microenvironment in diastole, which may be a more potent Ca^{2+} pool in activating calcineurin and CaMKII (22, 38, 39). Indeed, the T-tubule/RyR2 junctions align with sarcomeric Z-discs in which calcineurin/NFAT are anchored through calsarcin and α-actinin, suggesting they could directly sample Ca^{2+} in this microenvironment (40). Moreover, leaky RyRs in the heart associated with PKA/CaMKII activation and oxidation and nitrosylation, downstream of β-adrenergic signaling, are known disease determinants for hypertrophy and worsening heart failure (25, 41). This contention is entirely consistent with a recent report from Wehrens and colleagues, in which they made a RyR2 knockin mouse model that leaks Ca^{2+}, leading to greater cardiac hypertrophy and calcineurin/NFAT activation (42). Thus, enhanced β-receptor signaling and elevated resting Ca^{2+} in the cleft microenvironment due to RyR2 leak (or Ca^{2+} from another source) likely serve as interrelated effects, leading to a greater hypertrophic response in α1C-deleted mice. In addition, decreased Ca^{2+} influx via α1C could decrease Ca^{2+}-dependent inactivation of $I_{Ca\text{-}L}$ and thereby also contribute to increasing junctional cleft Ca^{2+} concentration. Indeed, we observed a significant elevation in the fast component of inactivation (τ_f) in both $\alpha 1C^{-/+}$ and $\alpha 1C^{-/fl\text{-}Cre}$ myocytes (Supplemental Figure 2).

The proposed elevation in resting Ca^{2+} in the RyR2 cleft microenvironment should render these channels more likely to open with less LTCC influx. Another means of accomplishing this compensatory alteration could be to change NCX1 activity. Indeed, deletion of NCX1 from the mouse heart led to a compensatory reduction of nearly 60% in LTCC current, while increased NCX1 activity in the heart, due to transgene-mediated overexpression, produced more LTCC current (43, 44). Moreover, LTCC activity directly influences NCX1 activity in the cleft microenvironment, leading to the hypothesis that reduced LTCC activity should produce less NCX1 activity, leading to increased cleft Ca^{2+} and increased gain in ECC (45). While we did not directly observe a change in NCX1 current from isolated adult cardiomyocytes from $\alpha 1C^{-/fl\text{-}Cre}$ mice, in vitro conditions are probably not appropriate to observe the proposed compensatory alterations that might result in less Ca^{2+} extrusion

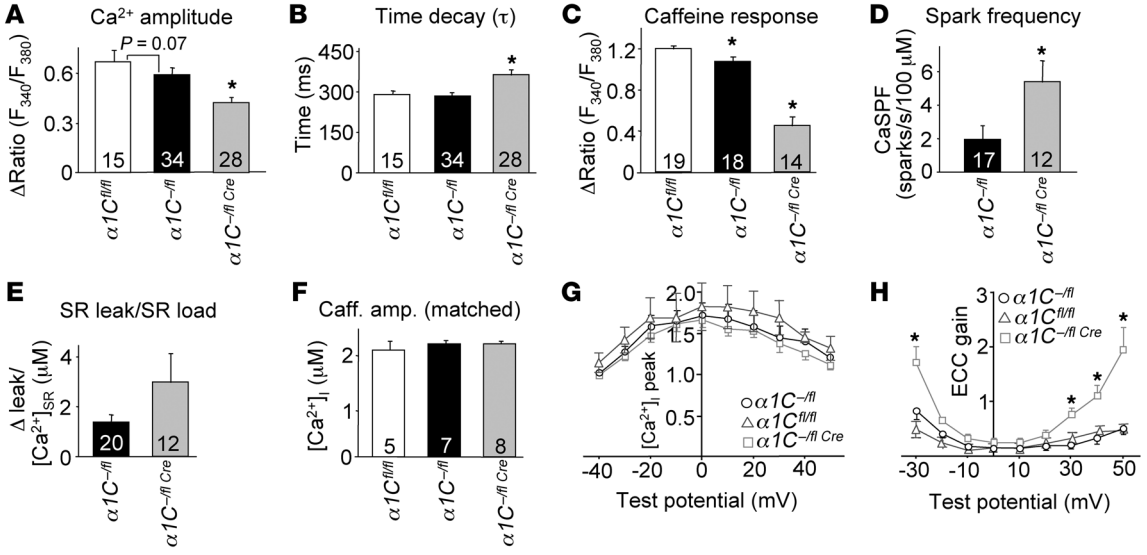

Figure 6

Ca^{2+} handling, SR Ca^{2+} leak, and increase in the gain of Ca^{2+}-induced Ca^{2+} release in α1C targeted mice. (**A** and **B**) Average maximal amplitude of electrically evoked Ca^{2+} transients and the Ca^{2+} decay time constant in adult cardiomyocytes from hearts of $\alpha 1C^{fl/fl}$, $\alpha 1C^{-/fl}$, and $\alpha 1C^{-/fl\text{-}Cre}$ mice. *$P < 0.05$ compared with $\alpha 1C^{-/fl}$. (**C**) Peak Ca^{2+} release after caffeine stimulation in myocytes from hearts of $\alpha 1C^{fl/fl}$, $\alpha 1C^{-/fl}$, and $\alpha 1C^{-/fl\text{-}Cre}$ mice. *$P < 0.05$ compared with $\alpha 1C^{-/fl}$. (**D**) SR Ca^{2+} spark measurements and (**E**) corresponding SR Ca^{2+} leak normalized to total SR Ca^{2+} content measured in cardiomyocytes from $\alpha 1C^{-/fl}$ and $\alpha 1C^{-/fl\text{-}Cre}$ mice. CaSPF, Ca^{2+} spark frequency. *$P < 0.05$ compared with $\alpha 1C^{-/fl}$. (**F**) Maximal caffeine-induced Ca^{2+} transients in SR Ca^{2+} load-matched myocytes used to measure gain of ECC. Caff. amp., caffeine amplitude. (**G**) Voltage dependence of intracellular Ca^{2+} transients in patch clamp experiments, simultaneously measuring $I_{Ca\text{-}L}$ and Ca^{2+} transients in $\alpha 1C^{fl/fl}$, $\alpha 1C^{-/fl}$, and $\alpha 1C^{-/fl\text{-}Cre}$ myocytes (SR load matched). (**H**) Gain of ECC calculated as a ratio of maximal $I_{Ca\text{-}L}$ and peak Ca^{2+} transient in myocytes shown in **F** and **G**. *$P < 0.05$ compared with control ($\alpha 1C^{-/fl}$ and $\alpha 1C^{fl/fl}$). The total number of myocytes used in each experimental group is shown on the bars in the graphs (from at least 3 mice for each genotype).

by NCX1 in vivo (Supplemental Figure 4). Finally, another compensatory alteration that might occur with reduced LTCC activity is through increased transient receptor potential canonical (TRPC) channel activity. Indeed, TRPC3 or TRPC6 overexpression in the heart induces Ca^{2+} influx, calcineurin activation, and mild hypertrophy (46, 47), and TRPC channels can functionally "couple" with LTCCs to alter each others' activity (48–50). TRPC channels were also shown to couple to RyR1 in skeletal muscle to induce Ca^{2+} release (51). Despite these relationships, we did not observe an increase in store-operated Ca^{2+} entry in cardiomyocytes from $\alpha 1C^{-/fl\text{-}Cre}$ mice, suggesting that TRPC channel activity was not affected, at least as suggested by the surrogate measure of store-operated entry (Supplemental Figure 4). It should also be noted that we did not observe an increase in TTCC expression in hearts from α1C-deleted mice (data not shown). Despite a lack of changes in these and other Ca^{2+} handling proteins and currents in α1C-deleted hearts, we did observe a mild increase in heart rate and a reduction in mean arterial blood pressure compared with those of control mice (Supplemental Figure 5).

While the ability to directly measure Ca^{2+} in the cleft microenvironment is lacking, many additional indirect lines of evidence support a mechanism whereby Ca^{2+} in this compartment is elevated and functions as the primary disease effector in α1C-deleted mice. First, metoprolol reversed manifestations of heart disease in $\alpha 1C^{-/+}$ mice, likely by antagonizing the neuroendocrine signaling machinery that enhances Ca^{2+} leak from RyR2 or that otherwise contributes to Ca^{2+} dysregulation secondary to CaMKII and PKA signaling. Second, augmentation in TTCC current with the α1G transgene rescued hypertrophy in α1C-deleted mice by providing more systolic Ca^{2+} (presumably then reducing diastolic Ca^{2+}), although these mice still developed heart failure and perished prematurely (Supplemental Figure 3). The simplest interpretation of these observations is that the additional peak Ca^{2+} release from TTCCs obviated the need for compensatory increases in cleft Ca^{2+}, though because the TTCC is not coupled in the same manner as the LTCC, it ultimately still resulted in lethality and arrhythmia. Third, despite dramatically reduced SR Ca^{2+} levels, direct measures of relative SR leak and SR Ca^{2+} sparks were enhanced in $\alpha 1C^{-/fl\text{-}Cre}$ mice, suggesting that conditions are appropriate for RyR2 leak. Fourth, calcineurin/NFAT signaling was dramatically increased in the hearts of $\alpha 1C^{-/fl\text{-}Cre}$ mice. Fifth, deletion of NCX1 in the heart, which also leads to a dramatic compensatory reduction in LTCC current (60%) (43), similarly led to much greater cardiac hypertrophy and dysfunction in young adult mice after TAC stimulation (45).

There may also be physiologic relevance to our results, such that LTCC current reductions might occur in the natural course of heart failure disease etiology. While it remains controversial whether LTCC current is reduced in cardiomyocytes from rats or humans with heart failure (15), there is general agreement that myocytes from failing human hearts show less β-adrenergic LTCC reserve (52). In the failing mouse heart, we reliably observed a significant ($P < 0.05$) reduction in α1C protein after 8 weeks of pressure overload stimulation (Supplemental Figure 6). Myocytes from these same WT hearts showed hypertrophy, a reduction in the Ca^{2+} transient, and a significant reduction in LTCC current (Supplemental Figure 6). Thus, a reduction in LTCC "function" (actual or reserve activity) may indeed be a physiologic consequence of heart

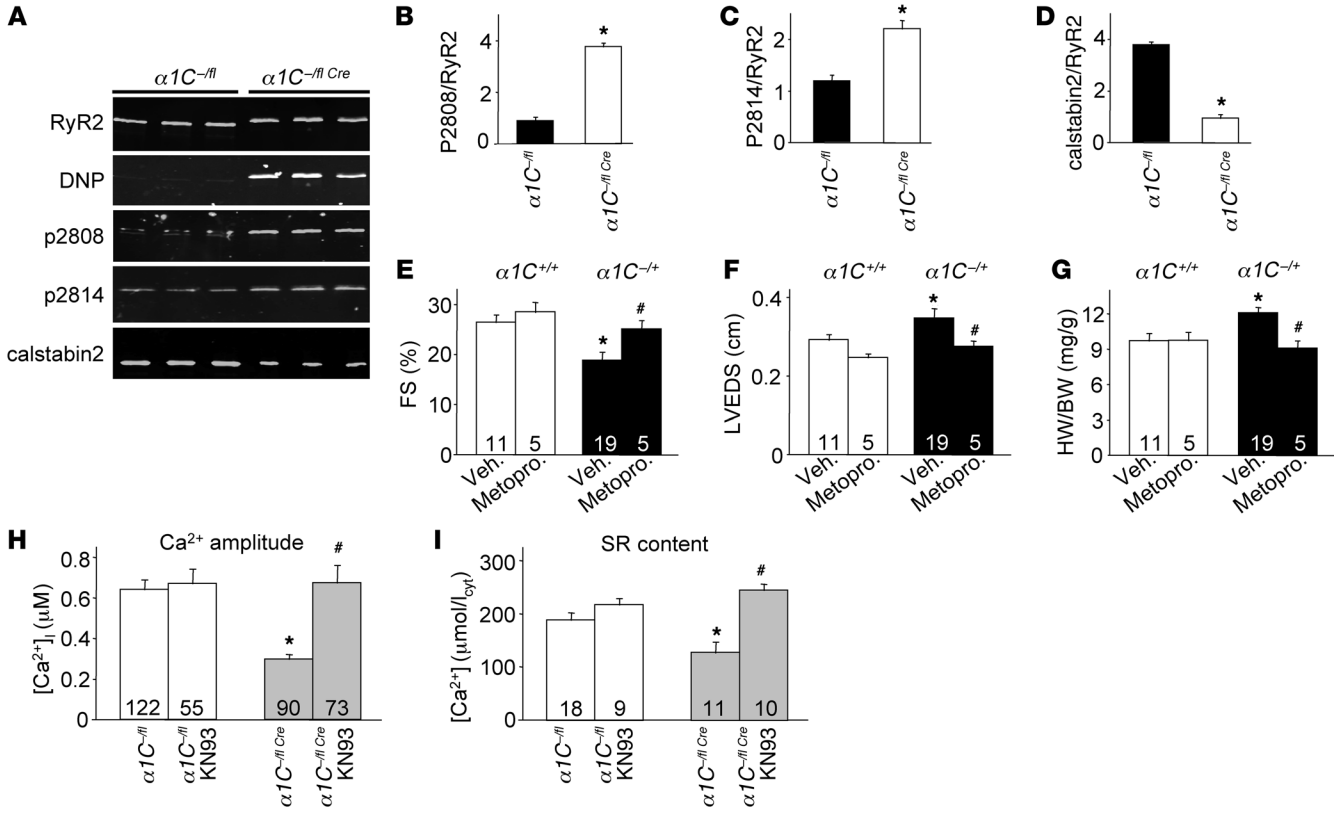

Figure 7

RyR2 phosphorylation and oxidation is increased, and blockade of β-adrenergic receptors prevents enhanced pathological responses in $\alpha 1C^{-/+}$ mice after pressure overload. (**A**–**D**) Western blotting and quantitation for calstabin2 and RyR2 levels from RyR2 immunoprecipitation samples as well as RyR2 phosphorylation at serine 2808 and 2814 and detection of oxidation and nitrosylation with 2,4-DNP reaction with the immunoprecipitate, followed by Western blotting with an anti-DNP antibody. $^{*}P < 0.05$ versus $\alpha 1C^{-/fl}$. (**E** and **F**) Echocardiographic assessment of FS and left ventricular end dimension at systole in $\alpha 1C^{-/+}$ and $\alpha 1C^{+/+}$ mice at 2 months of age after 2 weeks of pressure overload stimulation and treatment with metoprolol (metoprol) or vehicle. (**G**) HW/BW in the mice shown in **E**, after 2 weeks of pressure overload. (**E**–**G**) $^{*}P < 0.05$ compared with vehicle-treated $\alpha 1C^{+/+}$ mice; $^{\#}P < 0.05$ compared vehicle-treated $\alpha 1C^{-/+}$ mice. (**H** and **I**) Amplitude of the Ca^{2+} transient and SR Ca^{2+} content in adult myocytes isolated from hearts of the indicated mice, with or without KN93 addition. $^{*}P < 0.05$ compared $\alpha 1C^{-/fl}$; $^{\#}P < 0.05$ compared with $\alpha 1C^{-/fl\text{-}Cre}$. The number of cells analyzed is shown on the bars in the graphs.

failure, leading to the same increase in resting cleft Ca^{2+} through RyR2 leak, leading to secondary hypertrophy signaling. Interestingly, BAY K8644-induced maximal $I_{Ca\text{-}L}$ in $\alpha 1C^{-/fl\text{-}Cre}$ myocytes was significantly ($P < 0.001$) blunted compared with that of control myocytes (data not shown), similar to what has been shown in failing human ventricular myocytes (52). At the very minimum, our data at least suggest caution in applying LTCC antagonists for the treatment of heart failure, given the prominent disease-predisposing pathway that arose in the mouse with reduced cardiomyocyte-specific LTCC activity.

Methods

Animals. α1C gene-targeted mice were described previously as were α1C mice with targeted loxP sites to permit conditional gene deletion with Cre recombinase expression (7, 53). Transgenic mice expressing Cre recombinase or MerCreMer from the α-MHC promoter were described previously (54, 55). NFAT-luciferase, tetracycline transactivator, and cardiac-specific α1G overexpressing transgenic mice were described previously (27, 56, 57). Use of animals in this study was approved by the IACUC at the Cincinnati Children's Hospital Medical Center.

Western blot analysis. Western blot analysis was performed using mouse ventricles snap frozen in liquid nitrogen and stored at –70°C. Ventricles were homogenized in modified RIPA buffer, containing 50 mM Tris (pH 7.4), 150 mM NaCl, 0.25% sodium deoxycholate, 1 mM EDTA, and protease inhibitors. Homogenates were centrifuged at 20,817 *g* for 10 minutes, and the supernatants were used for blotting. Six to twenty-five micrograms of protein were loaded on 6%–15% SDS polyacrylamide gels suitable for detecting specific proteins relative to their molecular weights. Antibodies against the α1C subunit (Alamone Labs), α1G (NeuroMab), α1H (NeuroMab), α1D (NeuroMab), and GAPDH (Fitzgerald Industries International) were used. Chemifluorescence detection was performed with the Vistra ECF reagent (Amersham Pharmacia Biotech) and scanned with a Bio-Rad Gel Documentation center. For assessing RyR modifications, hearts were isotonically lysed in 1.0 ml of a buffer containing 50 mM Tris-HCl (pH 7.4), 20 mM NaF, 1.0 mM Na_3VO_4, and protease inhibitors. RyR2 was immunoprecipitated from the sample with a RyR2 antibody (4 μg Ab5029) in 1.0 ml of a modified RIPA buffer (50 mM Tris-HCl [pH 7.2], 0.9% NaCl, 5.0 mM NaF, 1.0 mM Na_3VO4, 1% Triton X-100, and protease inhibitors) for 1 hour at 4°C. The immune complexes were incubated with protein A Sepharose beads (Sigma-Aldrich) at 4°C for 1 hour, and the beads were

washed 3 times with RIPA buffer. To determine channel oxidation, the carbonyl groups in the protein side chains within the immunoprecipitate were derivatized to 2,4-dinitrophenylhydrazone (DNP-hydrazone) by reaction with 2,4-dinitrophenylhydrazine (Oxyblot Protein Oxidation Detection Kit, Millipore). Proteins were separated by SDS-PAGE (6% for RyR, 15% for calstabin) and transferred onto nitrocellulose membranes for 1 hour at 200 mA (SemiDry transfer blot, Bio-Rad). After incubation with blocking solution (LICOR Biosciences) to prevent nonspecific antibody binding, immunoblots were developed with an anti-RyR antibody (Affinity Bioreagents), RyR phospho-specific antibodies (RyR2-P2808 or RyR2-P2815; 1:5,000), or anti-calstabin (Santa Cruz Biotechnology Inc.). All immunoblots were developed and quantified using the Odyssey Infrared Imaging System (LICOR Biosystems) and infrared-labeled secondary antibodies.

Isolation of adult cardiomyocytes and Ca^{2+} measurements. Ca^{2+}-tolerant cardiomyocytes were selected after a standard isolation procedure from whole hearts placed in Tyrode solution with additives (120 mM NaCl, 5.4 mM KCl, 1.2 mM NaH_2PO_4, 5.6 mM glucose, 20 mM $NaHCO_3$, 1.6 mM $MgCl_2$, 10 mM 2,3-butanedione monoxime [BDM], and 5 mM taurine; buffer A). Hearts were then perfused with buffer containing liberase blendzyme (Roche) at 37°C (10–14 minutes total). After perfusion, the ventricles were disassociated into individual myocytes, filtered, and incubated with 2 μM Fura-2 acetoxymethyl ester (Invitrogen) and pluronic acid for 15 minutes in M199 media with BDM at room temperature. After loading, the cells were washed and resuspended in Ringer's solution. The photometry measurements were made in Ringer's solution using a DeltaRam spectrofluorophotometer (Photon Technology International), operated at an emission wavelength of 510 nm, with excitation wavelengths of 340 and 380 nm. The stimulating frequency for Ca^{2+} transient measurements was 0.5 Hz. Baseline amplitude (estimated by a 340 nm/380 nm ratio) of the Ca^{2+} signal was acquired, and data were analyzed using Felix and Clampfit software. SR Ca^{2+} leak and Ca^{2+} spark measurements were made as previously described (58, 59). Hearts were quickly excised and washed in chilled Ca^{2+}-free Tyrode solution, followed by retrograde perfusion with buffer containing collagenase II (Worthington) at 37°C for 6 to 10 minutes. The ventricles were subsequently dissociated into single myocytes and filtered, and Ca^{2+} was increased to reach a final level of 1.8 mM. Ca^{2+}-tolerant cells were then loaded with 1 μM Fluo4-AM and 20% pluronic acid (Invitrogen) for 30 minutes at room temperature. The myocytes were plated on glass cover slips coated with laminin (Invitrogen) and washed for 20 minutes to get rid of excess dye and to allow deesterification used for Ca^{2+} leak or spark measurements. For Ca^{2+} leak measurements, the coverslips were mounted on an inverted Nikon microscope and electrically stimulated at 0.5 Hz at least 20 times in 1.8 mM Ca^{2+} normal tyrode to reach steady state. Cells were excited at 490 ± 5 nm, and emission was recorded at 530 ± 20 nm. After stopping the stimulation, the solution was rapidly switched to a Na^+- and Ca^{2+}-free solution (140 mM LiCl, 1 mM $MgCl_2$, 4 mM CsCl, 10 mM HEPES, 1 mM EGTA, 10 mM glucose) for 30 seconds, so the Na^+-Ca^{2+} exchanger was blocked, and little or no Ca^{2+} could leave or enter the cell. One millimolar tetracaine (Sigma-Aldrich) was added to block the RyRs and thus inhibit leak from the SR. After 20 seconds, the solutions were switched back to Na^+- and Ca^{2+}-free tyrode for a duration of 10 seconds before 10 mM caffeine was added to deplete the Ca^{2+} stores. The difference in levels of baseline Ca^{2+} with and without tetracaine is considered Ca^{2+} leak, and the difference in levels between basal and peak total cytosolic Ca^{2+} transient in the presence of caffeine was an index of SR Ca^{2+} content. Ca^{2+} values were calculated based on the assumption of a diastolic Ca^{2+} value of 0.12 μM.

Ca^{2+} sparks were recorded with an Olympus Fluoview FV 1000 in line scan mode. The cells were stimulated at 0.5 Hz at least 20 times before stimulation was stopped, and sparks were recorded at rest. The fluorophore was excited with an argon laser at 488 nm, and emission maximum was recorded at 516 nm. Sparks were counted using a custom made algorithm (IDL, ITT Visual Information Solutions) and calculated as sparks/s/100 μm.

Measurement of $I_{Ca\text{-}L}$ using patch clamp methods. Patch clamp experiments were used to measure $I_{Ca\text{-}L}$ in myocytes. To isolate myocytes, after perfusion, the ventricles were separated from the atria, minced, and gently agitated in low Cl^-, high K^+ Kraft-Bruhe (KB) solution consisting of 50 mM glutamic acid, 40 mM KCl, 20 mM taurine, 20 mM KH_2PO_4, 3 mM $MgCl_2$, 10 mM glucose, 1 mM EGTA, and 10 mM HEPES (pH 7.4). The dissociated cells were filtered through a nylon mesh and stored at 4°C in KB solution until use. Only Ca^{2+}-tolerant cells with clear cross-striations and without spontaneous contractions or substantial granulation were selected for the experiments. All patch clamp experiments were conducted at room temperature (20°C–23°C) using a patch clamp amplifier (Axopatch200A; Axon Instruments). The recorded currents ($I_{Ca\text{-}L}$) were filtered at 2 kHz through a 4-pole low-pass Bessel filter and digitized at 5 kHz. The experiments were controlled using pClamp software (Axon Instruments) and analyzed using Clampfit. Current recordings were performed in bath solution superfused with the following Na^+-free solution: 2 mM $CaCl_2$, 5 mM 4-aminopyridine, 136 mM tetraethylammonium-Cl (TEA-Cl), 1.1 mM $MgCl_2$, 25 mM HEPES, and 22 mM glucose (pH 7.4 with TEA-OH). The pipette solution contained 100 mM cesium aspartate, 20 mM CsCl, 1 mM $MgCl_2$, 2 mM Mg-ATP, 0.5 mM Na_2-GTP, 5 mM EGTA, 5 mM HEPES (pH 7.3 with 1 N CsOH). $I_{Ca\text{-}L}$ was measured by applying depolarizing voltage steps (380 ms) –40 mV to +60 mV, respectively, in 10-mV increments.

ECC efficiency in both control and $\alpha 1C^{-/fl\text{-}Cre}$ myocytes was evaluated by simultaneous recording of $I_{Ca\text{-}L}$ and $[Ca^{2+}]_I$ with a whole-cell voltage clamp technique. Myocytes were placed in a chamber mounted on an inverted Nikon microscope and perfused with normal Tyrode salt solution containing 150 mM NaCl, 5.4 mM KCl, 1 mM $CaCl_2$, 1.2 mM $MgCl_2$, 10 mM glucose, 2 mM sodium pyruvate, and 5 mM HEPES (pH 7.4) at 35°C. The pipette solution was composed of salts: 120 mM Cs-aspartate, 10 mM NMDG, 20 mM TEA-Cl, 2.5 mM Tris-ATP, 0.05 mM Tris-GTP, and 5.4 mM KCl (pH 7.2 with CsOH). Na^+ currents were eliminated by holding the cell at –40 mV, and K^+ currents were suppressed by low intracellular K^+ and extracellular Cs^+ and intracellular TEA^+. ECC efficiency was studied in myocytes with matched SR Ca^{2+} load. For control myocytes, 10 consecutive depolarizations to +10 mV for 100 ms at 1 Hz were applied before each test potential, and, for $\alpha 1C^{-/fl\text{-}Cre}$ myocytes, 10 consecutive depolarizations to +10 mV for 400 ms were applied before each test potential. SR Ca^{2+} load was measured with a caffeine spritz, and peak caffeine-induced Ca^{2+} transient amplitude was considered as the index of SR Ca^{2+} content. Only cells with comparable SR load were used for data analysis. The gain of ECC was calculated by dividing the amplitude of Ca^{2+} transient by the amplitude of $I_{Ca\text{-}L}$ at each voltage.

To measure I_{NCX}, myocytes were depolarized to −45 mV from a holding potential of −90 mV to inactivate Na^+ current. The voltage was then stepped to +60 mV and ramped down to −90 mV to induce remaining currents. When steady state was reached, the protocol was repeated in the presence of 5 mM $NiCl_2$. I_{NCX} is defined as the nickel-sensitive current induced during the ramped potential. Pipette solutions contained 45 mM CsCl, 55 mM Cs-methanesulfonic acid, 10 mM ATP-Tris, 0.3 mM GTP-Tris, 20 mM HEPES, 5 mM BAPTA, 10.8 mM $MgCl_2$, 2.21 mM $CaCl_2$, and 14 mM NaCl (pH 7.3 with CsOH). Bath solution contained 137 mM NaCl, 1.0 mM $MgCl_2$, 5.4 mM CsCl, 1.0 mM $CaCl_2$, 10 mM dextrose, and 10 mM HEPES (pH 7.4 with NaOH) plus 10 μM nifedipine.

Echocardiography, drug treatment, swimming test, and pressure overload. Mice from all genotypes or treatment groups were anesthetized with isoflurane, and echocardiography was performed using a Hewlett Packard 5500

instrument with a 15-MHz microprobe. Echocardiographic measurements were taken on M-mode in triplicate for each mouse. For pressure overload, 10-week-old mice of each genotype were subjected to a TAC or sham surgical procedure as previously described (56). Pressure gradients across the constriction were measured by Doppler echocardiography as previously described (27). Alzet osmotic minipumps (no. 2002; Durect Corp.) containing Iso (60 mg/kg/d) or PBS were surgically inserted dorsally and subcutaneously in 2-month-old mice under isoflurane anesthesia. The β-adrenergic receptor antagonist metoprolol (2 g/ml, Sigma-Aldrich), diltiazem (450 mg/l, Sigma-Aldrich), and verapamil (400 mg/l, Sigma-Aldrich) were given in drinking water as previously reported (19, 29, 60). Swimming exercise protocol, which called for 21 days of exercise to induce physiological hypertrophy, was described previously (56). CsA (Sandimmune, Novartis) was administered subcutaneously twice daily at 10 mg/kg for 21 days.

Calcineurin activity assay. Phosphatase activity was measured by using the calcineurin assay kit (Enzo Life Sciences) according to the manufacturer's instructions. Cardiac lysates from either control or $\alpha 1C^{-/fl\text{-}Cre}$ mice were isolated, and calcineurin activity was measured as the dephosphorylation rate of a synthetic phosphopeptide substrate (RII peptide) in the presence or absence of EGTA. The amount of PO_4 release was determined photometrically by using the Biomol Green reagent (Enzo Life Sciences).

Statistics. All results are presented as mean ± SEM. Statistical analysis was performed with unpaired 2-tailed *t* test (for 2 groups) and 1-way ANOVA with Bonferroni correction (for groups of 3 or more). *P* values of less than 0.05 were considered significant.

Acknowledgments

This work was supported by grants from the NIH (to J.D. Molkentin, D.M. Bers, A.R. Marks, and S.R. Houser). J.D. Molkentin was also supported by the Howard Hughes Medical Institute. S.A. Goonasekera was supported by a local affiliate of the American Heart Association, R.N. Correll was supported by an NIH postdoctoral fellowship, and M. Auger-Messier was supported by Heart and Stroke Foundation of Canada.

Received for publication March 28, 2011, and accepted in revised form October 12, 2011.

Address correspondence to: Jeffery D. Molkentin, Cincinnati Children's Hospital Medical Center, Howard Hughes Medical Institute, Molecular Cardiovascular Biology, 240 Albert Sabin Way, MLC 7020, Cincinnati, Ohio 45229, USA. Phone: 513.636.3557; Fax: 513.636.5958; E-mail: jeff.molkentin@cchmc.org.

1. Benitah JP, Alvarez JL, Gomez AM. L-type Ca(2+) current in ventricular cardiomyocytes. *J Mol Cell Cardiol*. 2010;48(1):26–36.
2. Bers DM. Cardiac excitation-contraction coupling. *Nature*. 2002;415(6868):198–205.
3. Bodi I, Mikala G, Koch SE, Akhter SA, Schwartz A. The L-type calcium channel in the heart: the beat goes on. *J Clin Invest*. 2005;115(12):3306–3317.
4. Dolphin AC. Beta subunits of voltage-gated calcium channels. *J Bioenerg Biomembr*. 2003;35(6):599–620.
5. Davies A, Hendrich J, Van Minh AT, Wratten J, Douglas L, Dolphin AC. Functional biology of the alpha(2)delta subunits of voltage-gated calcium channels. *Trends Pharmacol Sci*. 2007;28(5):220–228.
6. Yang L, Katchman A, Morrow JP, Doshi D, Marx SO. Cardiac L-type calcium channel (Cav1.2) associates with {gamma} subunits. *FASEB J*. 2011;25(3):928–936.
7. Seisenberger C, et al. Functional embryonic cardiomyocytes after disruption of the L-type alpha1C (Cav1.2) calcium channel gene in the mouse. *J Biol Chem*. 2000;275(50):39193–39199.
8. Weissgerber P, et al. Reduced cardiac L-type Ca^{2+} current in Ca(V)beta2$^{-/-}$ embryos impairs cardiac development and contraction with secondary defects in vascular maturation. *Circ Res*. 2006;99(7):749–757.
9. Fabiato A. Calcium-induced release of calcium from the cardiac sarcoplasmic reticulum. *Am J Physiol*. 1983;245(1):C1–C14.
10. Chawla S, Hardingham GE, Quinn DR, Bading H. CBP: a signal-regulated transcriptional coactivator controlled by nuclear calcium and CaM kinase IV. *Science*. 1998;281(5382):1505–1509.
11. Molkentin JD, et al. A calcineurin-dependent transcriptional pathway for cardiac hypertrophy. *Cell*. 1998;93(2):215–228.
12. Puceat M, Vassort G. Signalling by protein kinase C isoforms in the heart. *Mol Cell Biochem*. 1996; 157(1–2):65–72.
13. Sulakhe PV, Vo XT. Regulation of phospholamban and troponin–I phosphorylation in the intact rat cardiomyocytes by adrenergic and cholinergic stimuli: roles of cyclic nucleotides, calcium, protein kinases and phosphatases and depolarization. *Mol Cell Biochem*. 1995;149–150:103–126.
14. Keung EC. Calcium current is increased in isolated adult myocytes from hypertrophied rat myocardium. *Circ Res*. 1989;64(4):753–763.
15. Richard S, Leclercq F, Lemaire S, Piot C, Nargeot J. Ca^{2+} currents in compensated hypertrophy and heart failure. *Cardiovasc Res*. 1998;37(2):300–311.
16. Mukherjee R, Spinale FG. L-type calcium channel abundance and function with cardiac hypertrophy and failure: a review. *J Mol Cell Cardiol*. 1998;30(10):1899–1916.
17. Liao Y, et al. Amlodipine ameliorates myocardial hypertrophy by inhibiting EGFR phosphorylation. *Biochem Biophys Res Commun*. 2005;327(4):1083–1087.
18. Liao Y, et al. Benidipine, a long-acting calcium channel blocker, inhibits cardiac remodeling in pressure-overloaded mice. *Cardiovasc Res*. 2005;65(4):879–888.
19. Semsarian C, et al. The L-type calcium channel inhibitor diltiazem prevents cardiomyopathy in a mouse model. *J Clin Invest*. 2002;109(8):1013–1020.
20. Mahe I, Chassany O, Grenard AS, Caulin C, Bergmann JF. Defining the role of calcium channel antagonists in heart failure due to systolic dysfunction. *Am J Cardiovasc Drugs*. 2003;3(1):33–41.
21. Chen X, et al. Calcium influx through Cav1.2 is a proximal signal for pathological cardiomyocyte hypertrophy. *J Mol Cell Cardiol*. 2011;50(3):460–470.
22. Dolmetsch RE, Lewis RS, Goodnow CC, Healy JI. Differential activation of transcription factors induced by Ca^{2+} response amplitude and duration. *Nature*. 1997;386(6627):855–858.
23. Saucerman JJ, Bers DM. Calmodulin mediates differential sensitivity of CaMKII and calcineurin to local Ca^{2+} in cardiac myocytes. *Biophys J*. 2008;95(10):4597–4612.
24. Kiowski W, Erne P, Bertel O, Bolli P, Buhler F. Acute and chronic sympathetic reflex activation and antihypertensive response to nifedipine. *J Am Coll Cardiol*. 1986;7(2):344–348.
25. Wehrens XH, Lehnart SE, Marks AR. Intracellular calcium release and cardiac disease. *Annu Rev Physiol*. 2005;67:69–98.
26. Curran J, Hinton MJ, Rios E, Bers DM, Shannon TR. Beta-adrenergic enhancement of sarcoplasmic reticulum calcium leak in cardiac myocytes is mediated by calcium/calmodulin-dependent protein kinase. *Circ Res*. 2007;100(3):391–398.
27. Nakayama H, et al. alpha1G-dependent T-type Ca^{2+} current antagonizes cardiac hypertrophy through a NOS3-dependent mechanism in mice. *J Clin Invest*. 2009;119(12):3787–3796.
28. Pitt GS, Dun W, Boyden PA. Remodeled cardiac calcium channels. *J Mol Cell Cardiol*. 2006;41(3):373–388.
29. Nakayama H, et al. Ca^{2+}- and mitochondrial-dependent cardiomyocyte necrosis as a primary mediator of heart failure. *J Clin Invest*. 2007;117(9):2431–2444.
30. Muth JN, Bodi I, Lewis W, Varadi G, Schwartz A. A Ca(2+)-dependent transgenic model of cardiac hypertrophy: A role for protein kinase Calpha. *Circulation*. 2001;103(1):140–147.
31. Wang S, et al. Dilated cardiomyopathy with increased SR Ca^{2+} loading preceded by a hypercontractile state and diastolic failure in the alpha(1C)TG mouse. *PLoS One*. 2009;4(1):e4133.
32. Cingolani E, et al. Gene therapy to inhibit the calcium channel beta subunit: physiological consequences and pathophysiological effects in models of cardiac hypertrophy. *Circ Res*. 2007;101(2):166–175.
33. Rosati B, et al. Robust L-type calcium current expression following heterozygous knockout of the Cav1.2 gene in the adult mouse heart. *J Physiol*. 2011;589(pt 13):3275–3288.
34. Furberg CD, Psaty BM, Meyer JV. Nifedipine. Dose-related increase in mortality in patients with coronary heart disease. *Circulation*. 1995;92(5):1326–1331.
35. de Vries RJ, van Veldhuisen DJ, Dunselman PH. Efficacy and safety of calcium channel blockers in heart failure: focus on recent trials with second-generation dihydropyridines. *Am Heart J*. 2000;139(2 pt 1):185–194.
36. Grimm M, Brown JH. Beta-adrenergic receptor signaling in the heart: role of CaMKII. *J Mol Cell Cardiol*. 2010;48(2):322–330.
37. Wehrens XH, Marks AR. Molecular determinants of altered contractility in heart failure. *Ann Med*. 2004;36 suppl 1:70–80.
38. Dolmetsch RE, Xu K, Lewis RS. Calcium oscillations increase the efficiency and specificity of gene expression. *Nature*. 1998;392(6679):933–936.
39. Tomida T, Hirose K, Takizawa A, Shibasaki F, Iino M. NFAT functions as a working memory of Ca^{2+} signals in decoding Ca^{2+} oscillation. *EMBO J*. 2003;22(15):3825–3832.
40. Frey N, Richardson JA, Olson EN. Calsarcins, a novel family of sarcomeric calcineurin-binding proteins. *Proc Natl Acad Sci U S A*. 2000; 97(26):14632–14637.
41. Currie S. Cardiac ryanodine receptor phosphoryla-

tion by CaM Kinase II: keeping the balance right. *Front Biosci*. 2009;14:5134–5156.
42. van Oort RJ, et al. Accelerated development of pressure overload-induced cardiac hypertrophy and dysfunction in an RyR2-R176Q knockin mouse model. *Hypertension*. 2010;55(4):932–938.
43. Pott C, Philipson KD, Goldhaber JI. Excitation-contraction coupling in Na^+-Ca^{2+} exchanger knockout mice: reduced transsarcolemmal Ca^{2+} flux. *Circ Res*. 2005;97(12):1288–1295.
44. Reuter H, Han T, Motter C, Philipson KD, Goldhaber JI. Mice overexpressing the cardiac sodium-calcium exchanger: defects in excitation-contraction coupling. *J Physiol*. 2004;554(pt 3):779–789.
45. Jordan MC, Henderson SA, Han T, Fishbein MC, Philipson KD, Roos KP. Myocardial function with reduced expression of the sodium-calcium exchanger. *J Card Fail*. 2010;16(9):786–796.
46. Kuwahara K, et al. TRPC6 fulfills a calcineurin signaling circuit during pathologic cardiac remodeling. *J Clin Invest*. 2006;116(12):3114–3126.
47. Nakayama H, Wilkin BJ, Bodi I, Molkentin JD. Calcineurin-dependent cardiomyopathy is activated by TRPC in the adult mouse heart. *FASEB J*. 2006;20(10):1660–1670.
48. Bouron A, Boisseau S, De Waard M, Peris L. Differential down-regulation of voltage-gated calcium channel currents by glutamate and BDNF in embryonic cortical neurons. *Eur J Neurosci*. 2006;24(3):699–708.
49. Soboloff J, Spassova M, Xu W, He LP, Cuesta N, Gill DL. Role of endogenous TRPC6 channels in Ca^{2+} signal generation in A7r5 smooth muscle cells. *J Biol Chem*. 2005;280(48):39786–39794.
50. Wang Y, Deng X, Hewavitharana T, Soboloff J, Gill DL. Stim, ORAI and TRPC channels in the control of calcium entry signals in smooth muscle. *Clin Exp Pharmacol Physiol*. 2008;35(9):1127–1133.
51. Lee EH, Cherednichenko G, Pessah IN, Allen PD. Functional coupling between TRPC3 and RyR1 regulates the expressions of key triadic proteins. *J Biol Chem*. 2006;281(15):10042–10048.
52. Chen X, Piacentino V 3rd, Furukawa S, Goldman B, Margulies KB, Houser SR. L-type Ca^{2+} channel density and regulation are altered in failing human ventricular myocytes and recover after support with mechanical assist devices. *Circ Res*. 2002;91(6):517–524.
53. Langwieser N, Christel CJ, Kleppisch T, Hofmann F, Wotjak CT, Moosmang S. Homeostatic switch in hebbian plasticity and fear learning after sustained loss of Cav1.2 calcium channels. *J Neurosci*. 2010;30(25):8367–8375.
54. Sohal DS, et al. Temporally regulated and tissue-specific gene manipulations in the adult and embryonic heart using a tamoxifen-inducible Cre protein. *Circ Res*. 2001;89(1):20–25.
55. Agah R, Frenkel PA, French BA, Michael LH, Overbeek PA, Schneider MD. Gene recombination in postmitotic cells. Targeted expression of Cre recombinase provokes cardiac-restricted, site-specific rearrangement in adult ventricular muscle in vivo. *J Clin Invest*. 1997;100(1):169–179.
56. Wilkins BJ, et al. Calcineurin/NFAT coupling participates in pathological, but not physiological, cardiac hypertrophy. *Circ Res*. 2004;94(1):110–118.
57. Sanbe A, Gulick J, Hanks MC, Liang Q, Osinska H, Robbins J. Reengineering inducible cardiac-specific transgenesis with an attenuated myosin heavy chain promoter. *Circ Res*. 2003;92(6):609–616.
58. Shannon TR, Ginsburg KS, Bers DM. Quantitative assessment of the SR Ca^{2+} leak-load relationship. *Circ Res*. 2002;91(7):594–600.
59. Ziolo MT, Katoh H, Bers DM. Positive and negative effects of nitric oxide on Ca(2+) sparks: influence of beta-adrenergic stimulation. *Am J Physiol Heart Circ Physiol*. 2001;281(6):H2295–H2303.
60. Harding VB, Jones LR, Lefkowitz RJ, Koch WJ, Rockman HA. Cardiac beta ARK1 inhibition prolongs survival and augments beta blocker therapy in a mouse model of severe heart failure. *Proc Natl Acad Sci U S A*. 2001;98(10):5809–5814.